ISSN 1949-8470 (online)

World Journal of *Radiology*

World J Radiol 2024 October 28; 16(10): 497-628

Published by Baishideng Publishing Group Inc

World Journal of Radiology

Contents

Monthly Volume 16 Number 10 October 28, 2024

REVIEW

ORIGINAL ARTICLE

Retrospective Study

CASE REPORT

World Journal of Radiology

Monthly Volume 16 Number 10 October 28, 2024

Contents

ABOUT COVER

Editorial Board Member of *World Journal of Radiology*, Dusan Dj Popovic, MD, PhD, FESBGH, Assistant Professor of Internal Medicine and Gastroenterohepatology, Research Assistant Professor, University of Belgrade, Faculty of Medicine, Department of Gastroenterology and Hepatology, Clinic for Internal Medicine, University Clinical Hospital Center "Dr Dragisa Misovic-Dedinje", Belgrade 11000, Serbia. dusan.popovic@med.bg.ac.rs

AIMS AND SCOPE

The primary aim of *World Journal of Radiology* (*WJR*, *World J Radiol*) is to provide scholars and readers from various fields of radiology with a platform to publish high-quality basic and clinical research articles and communicate their research findings online.

WJR mainly publishes articles reporting research results and findings obtained in the field of radiology and covering a wide range of topics including state of the art information on cardiopulmonary imaging, gastrointestinal imaging, genitourinary imaging, musculoskeletal imaging, neuroradiology/head and neck imaging, nuclear medicine and molecular imaging, pediatric imaging, vascular and interventional radiology, and women's imaging.

INDEXING/ABSTRACTING

The *WJR* is now abstracted and indexed in PubMed, PubMed Central, Emerging Sources Citation Index (Web of Science), Reference Citation Analysis, China Science and Technology Journal Database, and Superstar Journals Database. The 2024 Edition of Journal Citation Reports® cites the 2023 journal impact factor (JIF) for *WJR* as 1.4; JIF without journal self cites: 1.4; 5-year JIF: 1.8; JIF Rank: 132/204 in radiology, nuclear medicine and medical imaging; JIF Quartile: Q3; and 5-year JIF Quartile: Q3.

RESPONSIBLE EDITORS FOR THIS ISSUE

NAME OF JOURNAL
World Journal of Radiology

ISSN
ISSN 1949-8470 (online)

LAUNCH DATE
January 31, 2009

FREQUENCY
Monthly

EDITORS-IN-CHIEF
Thomas J Vogl

EDITORIAL BOARD MEMBERS
https://www.wjgnet.com/1949-8470/editorialboard.htm

PUBLICATION DATE
October 28, 2024

INSTRUCTIONS TO AUTHORS
https://www.wjgnet.com/bpg/gerinfo/204

GUIDELINES FOR ETHICS DOCUMENTS
https://www.wjgnet.com/bpg/GerInfo/287

GUIDELINES FOR NON-NATIVE SPEAKERS OF ENGLISH
https://www.wjgnet.com/bpg/gerinfo/240

PUBLICATION ETHICS
https://www.wjgnet.com/bpg/GerInfo/288

PUBLICATION MISCONDUCT
https://www.wjgnet.com/bpg/gerinfo/208

ARTICLE PROCESSING CHARGE
https://www.wjgnet.com/bpg/gerinfo/242

STEPS FOR SUBMITTING MANUSCRIPTS
https://www.wjgnet.com/bpg/GerInfo/239

ONLINE SUBMISSION
https://www.f6publishing.com

World Journal of Radiology

Submit a Manuscript: https://www.f6publishing.com

World J Radiol 2024 October 28; 16(10): 497-511

DOI: 10.4329/wjr.v16.i10.497

ISSN 1949-8470 (online)

REVIEW

Quantitative magnetic resonance imaging in prostate cancer: A review of current technology

Ankita Dhiman, Virendra Kumar, Chandan Jyoti Das

Specialty type: Radiology, nuclear medicine and medical imaging

Provenance and peer review: Invited article; Externally peer reviewed.

Peer-review model: Single blind

Peer-review report's classification
Scientific Quality: Grade C
Novelty: Grade B
Creativity or Innovation: Grade B
Scientific Significance: Grade B

P-Reviewer: Zhang JH

Received: May 14, 2024
Revised: September 26, 2024
Accepted: October 20, 2024
Published online: October 28, 2024
Processing time: 166 Days and 19.8 Hours

Ankita Dhiman, Chandan Jyoti Das, Department of Radiodiagnosis and Interventional Radiology, All India Institute of Medical Sciences, New Delhi 110029, Delhi, India

Virendra Kumar, Department of NMR & MRI Facility, All India Institute of Medical Sciences, New Delhi 110029, Delhi, India

Corresponding author: Chandan Jyoti Das, MD, PhD, Professor, Department of Radiodiagnosis and Interventional Radiology, All India Institute of Medical Sciences, Ansari Nagar, New Delhi 110029, Delhi, India. chandan.das@aiims.edu

Abstract

Prostate cancer (PCa) imaging forms an important part of PCa clinical management. Magnetic resonance imaging is the modality of choice for prostate imaging. Most of the current imaging assessment is qualitative *i.e.*, based on visual inspection and thus subjected to inter-observer disagreement. Quantitative imaging is better than qualitative assessment as it is more objective, and standardized, thus improving interobserver agreement. Apart from detecting PCa, few quantitative parameters may have potential to predict disease aggressiveness, and thus can be used for prognosis and deciding the course of management. There are various magnetic resonance imaging-based quantitative parameters and few of them are already part of PIRADS v.2.1. However, there are many other parameters that are under study and need further validation by rigorous multicenter studies before recommending them for routine clinical practice. This review intends to discuss the existing quantitative methods, recent developments, and novel techniques in detail.

Key Words: Prostate cancer; Quantitative imaging; Magnetic resonance imaging; Apparent diffusion coefficient

Core Tip: Quantitative imaging has many advantages over conventional qualitative assessment. A few parameters have also been shown to correlate with the Gleason score and can help in deciding disease prognosis and clinical management. A quantitative imaging biomarker could improve prostate cancer (PCa) detection by minimizing inter-observer variability, thereby reducing overdiagnosis of clinically insignificant PCa (Gleason score < 7). This would help avoid unnecessary biopsies and decrease the overtreatment of slow-growing PCa. In addition, with further advancement in the quantitative imaging parameters, they may be used to monitor therapeutic response or to predict response to a particular treatment.

Citation: Dhiman A, Kumar V, Das CJ. Quantitative magnetic resonance imaging in prostate cancer: A review of current technology. *World J Radiol* 2024; 16(10): 497-511
URL: https://www.wjgnet.com/1949-8470/full/v16/i10/497.htm
DOI: https://dx.doi.org/10.4329/wjr.v16.i10.497

INTRODUCTION

Prostate cancer (PCa) is the second most common malignancy and one of the main causes of cancer related mortalities in males around the globe[1]. Traditional diagnostic methods like digital rectal examination, prostate specific antigen tests, and transrectal ultrasound (US)-guided biopsy have poor sensitivity and specificity and face limitations in staging and grading of PCa. Therefore, for better prognosis effective management, and treatment planning, accurate characterization of PCa is necessary[2].

Current imaging modalities available for imaging of PCa are transrectal US, multiparametric magnetic resonance imaging (MRI), positron emission tomography-computed tomography (PET-CT) scan, and PET-MRI (PET-MRI) scan. US plays a limited role in cancer detection as very small proportion of hypoechoic lesions are revealed to be tumors upon biopsy. Thus, it is used to visualize the prostate during transrectal or trans-perineal US-guided biopsies. CT offers high specificity in detecting very high-grade tumors but is still not ideal for diagnosing PCa as it lacks soft tissue resolution and molecular insights needed for accurate PCa detection[3]. PET scan uses a tracer to target prostate-specific membrane antigen which helps to detect lymph node metastasis in men with high-risk PCa. Prostate-specific membrane antigen PET has proven to be more effective than conventional CT in accurately staging high-risk PCa patients[4]. MRI, is a non-ninvasive method that integrates functional and morphological information to provide a superior soft-tissue contrast resolution, which permits resolution of intra-prostatic anatomy, discrimination of the prostate capsule, and differentiation of benign from malignant intraprostatic abnormalities which the other mentioned imaging techniques often lack[5].

Imaging modalities may provide structural as well as functional information, depending upon the modality and technique. However, most of the imaging assessment is qualitative *i.e.*, based on visual inspection and thus subjected to inter-observer disagreement. To overcome this and to enhance the objectivity of reporting, quantitative imaging techniques have been recommended which may play a major role. Quantitative imaging aims to assign a numerical value to the observations enabling higher accuracy, reproducibility, standardized reporting, interpretation, and communication. Few such MRI quantitative metrics are already part of PIRADS v.2.1[6]. However, many are still under study and need further validation. This review intends to discuss the existing quantitative methods, recent developments, and novel techniques in detail.

QUANTITATIVE PARAMETERS

Apparent diffusion coefficient

Diffusion-weighted imaging (DWI) is an important part of multiparametric MRI and enables the assessment of changes associate with the tissue organization in progression of PCa. High cellularity tissues by virtue of reduced extracellular space restrict the Brownian movement of water molecules and thus demonstrate diffusion restriction[7]. DWI acquisition sequence can be used to obtain two sets of images: (1) Diffusion weighted imaging acquired at different *b*-values, where, *b*-value signifies diffusion sensitizing gradient's strength with its unit being seconds/mm^2[8-10]; and (2) Apparent diffusion coefficient (ADC) map generated from the diffusion weighted images acquired at least two different *b*-values. When the logarithm of signal intensity decay on the Y-axis is plotted against *b*-values on the X-axis, the slope of the line which is produced represents the ADC value[7,9,10]. A minimum of two *b*-values are required for the calculation of ADC. DWI acquired at more than two *b*-values enhance the precision of ADC estimation at the cost of increased acquisition time[7]. There is a lack of standardization of number of *b*-values and highest *b*-value to use, which leads to differences in the calculation of ADC values. Many recent studies have proven the superiority of high *b*-value DWI (1500-2500 s/mm^2) over conventional DWI (b = 1000 s/mm^2)[11-18]. However, the disadvantage of a high *b* value includes a reduced signal-to-noise ratio, more susceptibility artifacts, and image distortion[19]. Specific software is also required for ADC calculation if using such high *b*-value[20]. Thus, routinely most of the centers prefer conventional DWI. PIRADS v.2.1 guidelines also recommend the use of *b* values ≤ 1000 s/mm^2[21].

Under PIRADS v.2.1, DWI is the primary sequence for assessing peripheral zone (PZ) lesions and a secondary sequence for transitional zone (TZ) lesions[22]. Low ADC values have been reported in TZ in benign stromal hyperplastic

nodules, which is the reason for not using DWI as a primary sequence for TZ[22]. Few studies have demonstrated higher ADC values in stromal hyperplastic nodules as compared to PCa, however, there is no clear-cut value to distinguish both and thus the use of quantitative ADC in the diagnosis of PCa in TZ is still not validated. DWI provides both qualitative (by assessing whether the tissue in question is showing restriction or not) and quantitative assessment. Various quantification metrics which are being explored include mean ADC, ADC ratio, ADC minimum, and histogram analysis. Currently, mean ADC is the only quantitative DWI parameter included under PIRADS v.2.1. Available literature has shown that the mean ADC value has an inverse relation with histological Gleason's score and thus it can be used to predict whether the prostate malignancy is high grade or low grade[23-25]. Lucarelli *et al*[5] showed that the mean ADC values decrease from International Society of Urological Pathology (ISUP) 2 to ISUP 5 showing significant differences between low, intermediate, and high-grade tumors. ADC values showed a strong positive correlation with ISUP groups in both the peripheral and transition zones; however, the correlation between ADC values and PIRADS groups is less reliable in the transition zone than in the peripheral zone[5]. One major limitation of mean ADC is averaging ADC values and masking of low ADC pixels which contain more aggressive tumor foci[26]. Also, there are no clear cut-off mean ADC values for benign and malignant lesions, as ADC value is highly influenced by many factors including the type of scanner used, *b*-values, physiological differences in background prostate tissue, *etc*[27-30]. To compensate for these differences, some authors have advised the use of ADC ratio which is defined as the ADC value of the prostatic area suspicious of malignancy divided by the ADC value in the non-malignant reference area[31-33]. There is no validated reference with respect to which ADC ratio should be calculated, different studies have used different references including normal TZ, and PZ, and some have also used urinary bladder as a reference[33,34]. The advantage of this method is that with no additional scan time, it allows lesion visualization by providing a highly diffusion-weighted image[35]. Also, there are two schools of thought on how to draw region of interest (ROI) for ADC ratio calculation. One group used ROI covering ADC minimum area[23,36] yielding ADC minimum ratio and another group advocated ROI covering whole lesion yielding ADC mean ratio[37,38]. A study compared both and found that ADC mean and the resulting ADC mean ratio was significantly better compared to ADC minimum and resulting ADC minimum ratio in discriminating high-grade from low-grade PCa[33].

ADC minimum and ADC histogram analysis have been proposed as two quantitative DWI methods which are beneficial especially in heterogeneous lesions[26,39]. ADC minimum is more sensitive to detecting aggressive tumor foci in a heterogenous mass with varying ADC values[40]. And, thus can act as a better targeting guide in prostatic biopsies. However, there is mixed data, as to whether ADC mean or ADC minimum correlates better with Gleason score (GS)[26,39,41]. The limitation of minimum ADC is being restrictive and more prone to fallacious due to artifacts[33,40,42]. Also as already discussed, ADC mean values due to averaging can mask the areas with minimum values, thus can underestimate the aggressiveness in a heterogenous lesion. To overcome this, some authors have come up with the concept of histogram analysis. Homogenous composition tumors will have the gaussian type of distribution as opposed to skewed distribution in heterogenous lesions[26]. The low centile values in the histogram have been shown to correlate better with GS[26,39,41]. However, the optimal centile that should be taken for analysis lacks standardization[36,42].

Tumor size and tumor volume by three-dimensional ellipsoid fit

Tumor size is an important part of the decision tree of PIRADS v.2.1 and the 15 mm cut-off differentiates PIRADS 4 from PIRADS 5 lesion[6] (Figure 1). This has been independently validated by many investigators. The measurement of the single longest diameter is easy to perform and has a good positive correlation with tumor volume (TV) at radical prostatectomy[43].

TV is associated with the prognosis of PCa[44,45]. TV more than 0.5 cm^3 is considered the threshold for significant disease[46]. Index lesion volume helps in deciding management, and guiding focal treatment, and is a good criterion for follow-up during active surveillance[47,48]. Focal therapy options such as high intensity focused US, cryotherapy, laser ablation, brachytherapy, electroporation, and radiofrequency ablation[49] require precise assessment of TV so that maximum energy is deposited in the cancerous tissue with minimal damage to the adjacent normal area[50,51]. Studies have found that pathological TV correlates with pathological stage and GS[43,44,52,53]. So, if TV on imaging can truly represent the pathological volume, it will also show a similar correlation with GS. A study by McNeal *et al*[54] demonstrated that if TV is less than 4 cm^3 the disease is usually confined to the prostate, and when TV is more than 12 cm^3 there is a high likelihood of distant metastasis. TV also correlates with the presence of vascular invasion and seminal vesicle involvement[55]. Many studies have shown that TV is better measured on ADC image as compared to other sequences, as ADC image best demarcates the margin of the lesion in contrast with the adjacent normal tissue[25,56]. A study also advocated an ADC value of 0.0016 mm^2/second as the cut-off for accurate measurement of TV (49)[57]. PIRADS v.2.1 assessment includes only the two-dimensional method for TV measurement. However, the drawback of using one of the most widely used two-dimensional conventional formulae for TV calculation *i.e.*, the ellipsoid formula is that it is a linear measurement based on the assumption of the lesion being of ellipsoid shape and does not take into account the irregular tumor shape (48)[58]. Three-dimensional measurement techniques of TV have not been thoroughly investigated. TV estimation by the ellipsoid fitting model has the potential to measure the tumor maximum dimension and TV accurately and may upgrade the PIRADS score (Figure 2) from 4 to score 5 (48)[58].

Shape analysis

Shape analysis is one of the potential quantitative parameters, which can have an important role in staging and prognosis [59]. Currently, PIRADS V2.1 includes only qualitative shape criteria, which are separate for TZ and PZ lesions. In TZ, lenticular shape favors malignancy, while round or oval shape favors benign prostatic hyperplasia (BPH)[22,60,61]. While for PZ, wedge, linear, shape, bandlike, diffuse shape have been described to occur more frequently in benign conditions, on the other hand, round or oval shape has been associated with PCa[22,62] (Figure 3). Shape assessment is done on DWI

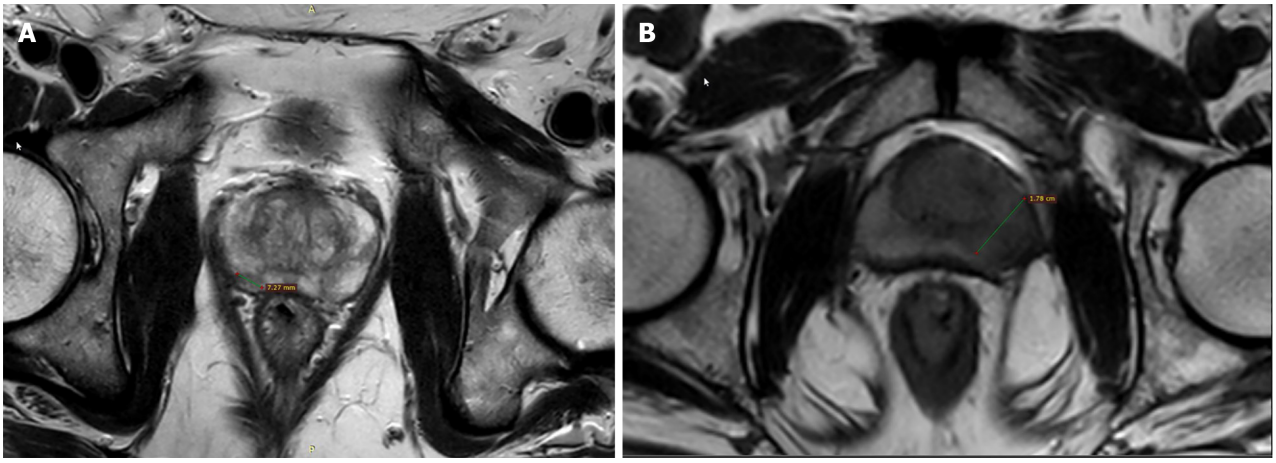

Figure 1 PIRADS 4 *vs* PIRADS 5 lesions on basis of size: T2 weighted axial image. A: A right peripheral zone ill-defined hypointense lesion measuring 727 mm suggestive of PIRADS 4 lesion; B: T2 weighted axial image showing a left peripheral zone ill-defined hypointense lesion measuring 17 cm suggestive of PIRADS 5 lesion.

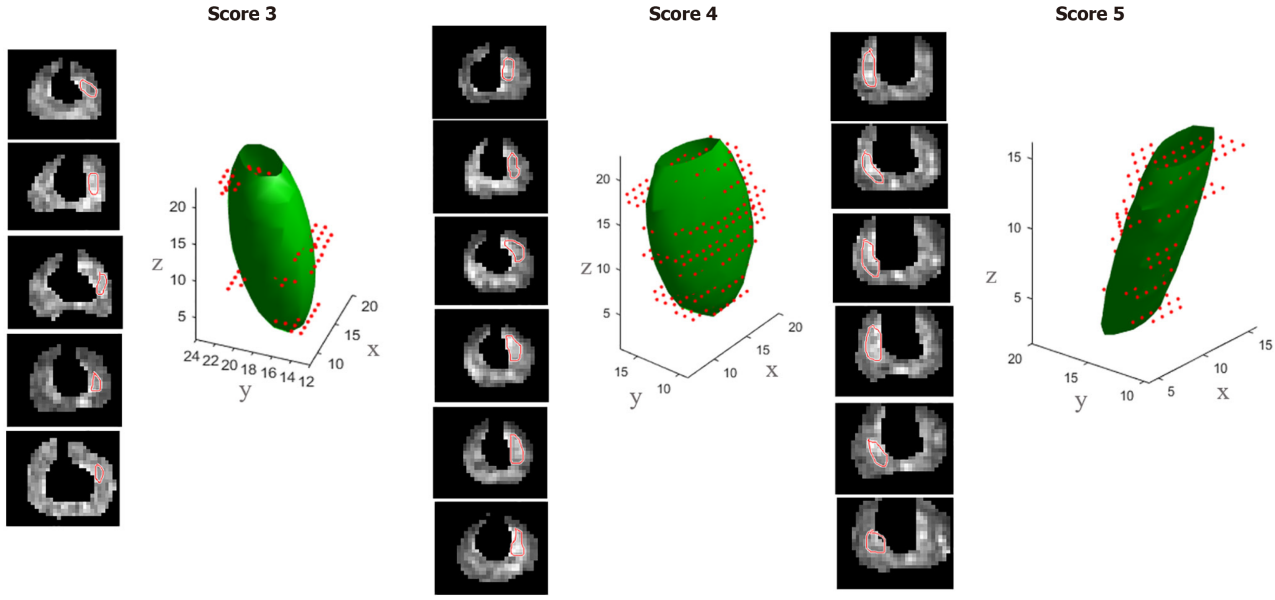

Figure 2 Three-dimensional ellipsoid fit: Three-dimensional fitting of the segmented lesions from. Diffusion-weighted magnetic resonance images (b = 2000 s/mm^2) for different PI-RADS scores.

sequence for PZ lesions[6] and on T2 sequence for TZ lesions[6]. Realizing the important role of shape analysis for PZ lesions, PIRADS v.2.1 has incorporated shape analysis of PZ lesions as well into decision making, while it was not included in the PIRADS V 2[6,22,60]. Various studies have been done to validate the importance of shape analysis in TZ and PZ lesions. In a study by Li *et al*[63], the ability of radiological semantics to discriminate clinically significant PCa (CsPCa) was studied on multiparametric MRI and it was found that kappa score for qualitative shape analysis showed only moderate interobserver agreement. In another shape metrics study for PZ tumors on DWI in 241 patients, the agreement of shape assessment was also moderate. The round or oval shape of the tumor was associated with a higher GS as compared to crescentic tumors and linear or wedge-shaped tumors (P = 0.011). In addition, tumors with round or oval shapes showed a greater degree of extracapsular extension (ECE) and seminal vesicle invasion[64] (extracapsular extension and seminal vesicle invasion: 70.1% and 26.0%) as compared to crescentic tumors (67.3% and 9.1%; P = 0.003) and linear or wedge-shaped tumors (40.6% and 9.4%; P = 0.008)[64]. Quantitative descriptors used for round and oval lesions were roundness and circularity, which were associated with more aggressive PCa[64]. A quantitative shape analysis study by Krishna *et al*[65] on TZ lesions on T2-weighted imaging compared it with subjective shape analysis. Circularity (correlating with round lesions) and convexity (correlating with lentiform lesions) shape features showed excellent inter reader agreement in differentiating TZ PCa and BPH; however, the quantitative feature representing lesion topology (number of spiculations) was not able to differentiate TZ PCa and BPH and was and thus inferior in accuracy than subjective shape analysis. In a study, it was shown that an advanced radiomic feature derived from an ADC map known as the surface area to volume ratio came out as a highly accurate and promising tool in discriminating CsPCa from non-CsPCa, and even outperforming previously described parameters such as TV and maximum diameter (5,7)[66].

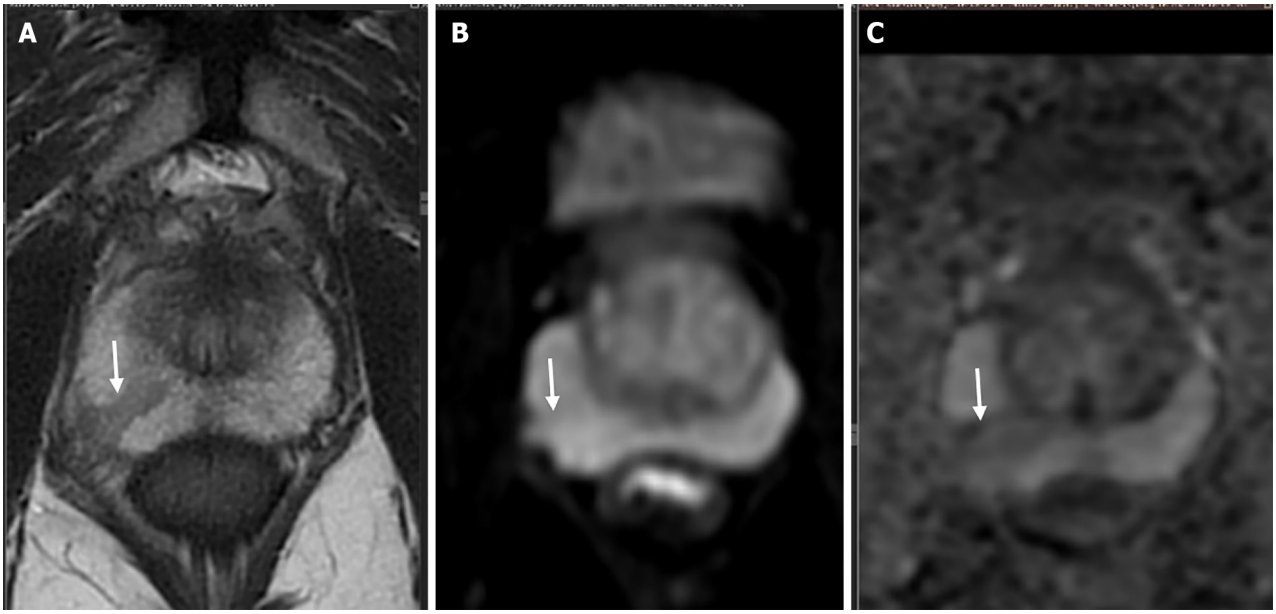

Figure 3 Shape analysis. A-C: T2-weighted axial image shows a wedge-shaped T2 hypointense lesion (arrow in A) in right peripheral zone which shows no diffusion restriction (arrow in B and C) is scored as a category 2 observation according to PIRADS v.2.1.

Length of capsular contact

Length of capsular contact (LCC) is the length for which the prostatic tumor is in contact with the prostatic capsule[67]. It is a simple measurement, relatively independent of the radiologist's experience, and more objective with good inter-reader reproducibility. This makes it a good quantitative criterion for diagnosing ECE, which is a crucial point in PCa staging and prognosis[68] (Figure 4). ECE in patients with T3bN0 PCa is linked with a greater risk of systemic spread of the disease and mortality. The presence of ECE is also an important treatment deciding point. If present, it upgrades the disease stage from T2 (organ-confined disease) to T3a (locally advanced disease)[68]. The curative treatment is most likely if the stage is ≤ T2c[69]. Currently, the criteria being used for diagnosing ECE in PIRADS v.2.1 include abutment or bulging of the capsule, irregularity of prostatic capsule, adjacent neurovascular bundle thickening, invasion of peri-prostatic fatty tissue and obliteration of the recto-prostatic angle[70]. However, these criteria are subjective and the reader's experience profoundly affects ECE detection as shown in a study by Wibmer *et al*[68]. Also, these criteria diagnose visible macroscopic ECE, not microscopic one[70]. Thus, there should be some relatively more objective criterion such as LCC to overcome the shortcomings of above listed subjective criteria.

LCC is found to be an independent and reproducible predictor of ECE in multiple studies[67,71-73]. In a study by Baco *et al*[67], the logistic regression analysis revealed that the pathological-LCC (0.821) superiorly correlated with microscopic ECE as compared to the pathological cancer volume (0.685). Spearman correlation between the pathological-LCC and MRI-LCC was significant with $r = 0.839$ ($P < 0.0001$). MRI-LCC threshold of 20 mm showed superior accuracy compared to subjective analysis in diagnosing microscopic ECE (82% *vs* 67%, $P = 0.015$). This concludes that LCC can outperform subjective criteria in predicting microscopic ECE. A meta-analysis by Kim *et al*[74] concluded, the more the MRI-LCC value, the higher is the probability of ECE. In a cohort study[75], LCC was found to be an independent predictor of pathological lymph node, and biochemical recurrence along with pathological ECE. A retrospective study also found, LCC and ADC when used in combination, improved the diagnostic performance in demonstrating microscopic ECE[76]. Limitations of LCC are the inter-individual differences in measurement technique (by linear or curvilinear method)[72,73], no defined threshold (varying between 6-20 mm)[72,76,77], no consensus on which sequence to be used for measurement. These points need further validation before its integration into routine clinical practice.

Dynamic contrast-enhanced MRI-based parameters (Ktrans, Kep)

Angiogenesis is considered as a hallmark of any malignancy including PCa and dynamic contrast-enhanced (DCE) imaging enables non-invasive assessment of tissue vascularity at the cellular level. And by assessing that, it has the potential to assess the aggressiveness of the tumor[24,78-81]. In PIRADS v.2.1, DCE imaging has accessory role as compared to the primary sequences such as T2 in TZ and DWI in PZ. Its main role is in PZ PIRADS 3 lesion, positive finding on DCE MRI upgrades score to PIRADS 4[22]. Lack of quantification is one of the major reasons behind its diminished role in PIRADS and quantification can help in utilizing the full potential of this technique. DCE is a functional imaging technique that offers qualitative, semiquantitative as well as quantitative assessment of PCa[82] (Figure 5). Quantitative assessment is preferred, as it provides objective reproducible numerical values and commutation is also easy these days due to easy availability of software packages. Quantitative kinetic parameters encompass Ktrans (volume transfer constant) and Kep (rate constant). Ktrans is equal to the product of permeability and surface area (P × S) per unit volume of the tissue[82]. Kep (Ktrans/Ve), refers to the efflux of contrast from the extracellular compartment back into plasma (Ve refers to extracellular extravascular volume fraction)[82]. A retrospective study of PZ lesions at 3T found a

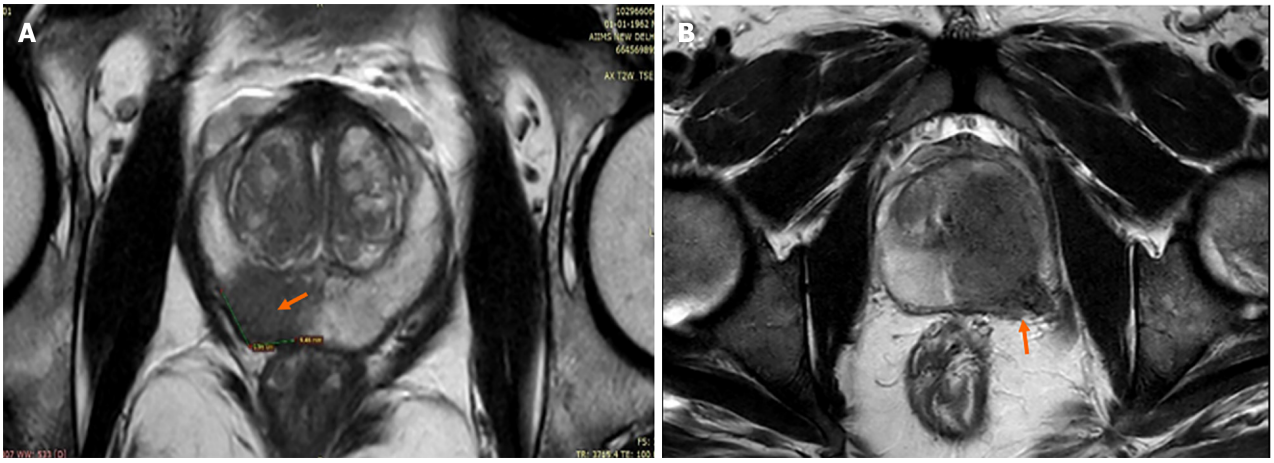

Figure 4 Length of capsular contact. A: T2-weighted axial image shows T2 hypointense lesion in right peripheral zone having wide contact (9.6 mm) with the capsule *i.e.*, wider length of capsular contact suggesting the possibility of microscopic capsular invasion which was confirmed on histopathology along with its high grade (Gleason score 4 + 5); B: T2-weighted axial image in another case shows T2 hypointense lesion in left transitional and peripheral zone having wide contact with capsule *i.e.*, wider length of capsular contact with adjacent neurovascular invasion (arrow).

significant correlation between Ktrans, Kep values, and aggressiveness of PCa[83]. The quantitative DCE parameters, Ktrans and Kep are highly correlated with the histopathology of the prostate tumor tissue and act as independent predictors of malignancy. Higher the Ktrans and Kep values, the lesion is more likely to be malignant. The study identified cutoff points of ± 0.2905 for Ktrans and ± 0.3365 for Kep, with sensitivities of 88.2% and 94.1%, specificities of 84.6% for both, positive predictive values of 88.2% and 88.9%, and negative predictive values (NPV) of 84.6% and 91.7%, respectively[84]. Few studies have also assessed the combined diagnostic accuracy of DCE with diffusion tensor imaging (DTI)[85] and also DCE with DWI[86] in PCa diagnosis. The combination helps in assessing different facets of the disease process, DCE assesses the micro-vessel density and permeability, while DTI and diffusion focus on cellular density. One such study by Li *et al*[85] in PZ lesions on 3T MRI found that DTI + DCE was significantly better than either DTI [area under the receiver operating characteristic curve (AUC) 0.93 *vs* 0.86, $P = 0.0017$] or DCE (AUC 0.93 *vs* 0.84, $P = 0.0034$) alone. On the contrary, many studies have also found an overlap of Ktrans and Kep values for benign and malignant lesions[87,88] and also there are studies that demonstrated no correlation between any of the DCE parameters and GS [89]. The study performed by Feng *et al*[90], showed that as a single predictor DCE [the odds ratios (OR) of Kep (0.987, $P > 0.05$) and Ktrans (0.794, $P > 0.05$) closer to 1] does not contribute to the CsPCa model. However, the diagnostic and positive predictive value of the multiparametric model were significantly higher than those of the biparametric model (prostate MRI without DCE)[90]. This concludes DCE should be interpreted always in conjunction with other MRI parameters for better results.

Intravoxel incoherent motion and Kurtosis

Le Bihan *et al*[91] and Le Bihan[92] first introduced the concept of intravoxel incoherent motion (IVIM), merging the diffusion and perfusion components, for quantitative analysis of the microstructure and microvasculature of the tissue. It is an extended version of DWI and can be used in the detection of PCa in PZ and TZ. DWI is based on the mono-exponential decay theory, assuming the gaussian distribution of Brownian motion of water molecules. However, such an assumption doesn't always hold true in vivo, where countless numbers of barriers and inter and intracellular compartments restrict diffusion. This leads to non-gaussian distribution pattern[93,94]. IVIM tries to capture this intravoxel diffusion heterogeneity of the tumor. Multiple *b*-values ranging from 0 to 2000 s/mm^2 are used. A study by Malagi *et al* [95] concluded that a combination of 8 *b* values provides reasonably good accuracy in IVIM parameters. IVIM is based on a bi-exponential model and yields pure diffusion parameters (D) and perfusion-related diffusion parameters (D* is perfusion-related diffusion coefficient and f is perfusion fraction) (Figure 6). Kurtosis imaging is another upgradation of conventional DWI, which utilizes kurtosis-based diffusion model to characterize the multiexponential behavior of diffusion decay. IVIM-diffusion kurtosis imaging (DKI) model is traditionally a 3 T model. However, a study by Malagi *et al*[96] demonstrated that using an advanced spatial penalty-based reconstruction method on 1.5 T can be used as an alternative to 3 T with fewer estimation errors in distinguishing PCa and BPH.

Previous studies demonstrated that IVIM parameters were inferior to ADC in the evaluation of TZ lesions[97]; however, could increase the diagnostic yield in PZ lesions[95]. A study by Chang *et al*[98], found that D mean and D*kurtosis were important predictors of the postoperative ISUP high-risk group ($P < 0.05$). Liu *et al*[99] in comparison of the following models *i.e.*, the monoexponential model (conventional DWI), IVIM, IVIM kurtosis, and kurtosis model, found that each model was useful for PCa diagnosis, however, diagnostic efficacy was similar amongst them. A recent study by Das *et al*[100] evaluated the role of combined IVIM-DKI and their machine-learning-based texture analysis (TA) for the detection and assessment of severity in PCa. The results of the study reported that D, f, and k computed using the IVIM-DKI model with the TV method were able to differentiate PCa from BPH and normal PZ. Texture features of combined IVIM-DKI parameters showed high accuracy and AUC in PCa detection[100]. Few studies have also demonstrated that D performed better than ADC and other parameters in distinguishing high-grade and low-grade PCa[95,101-

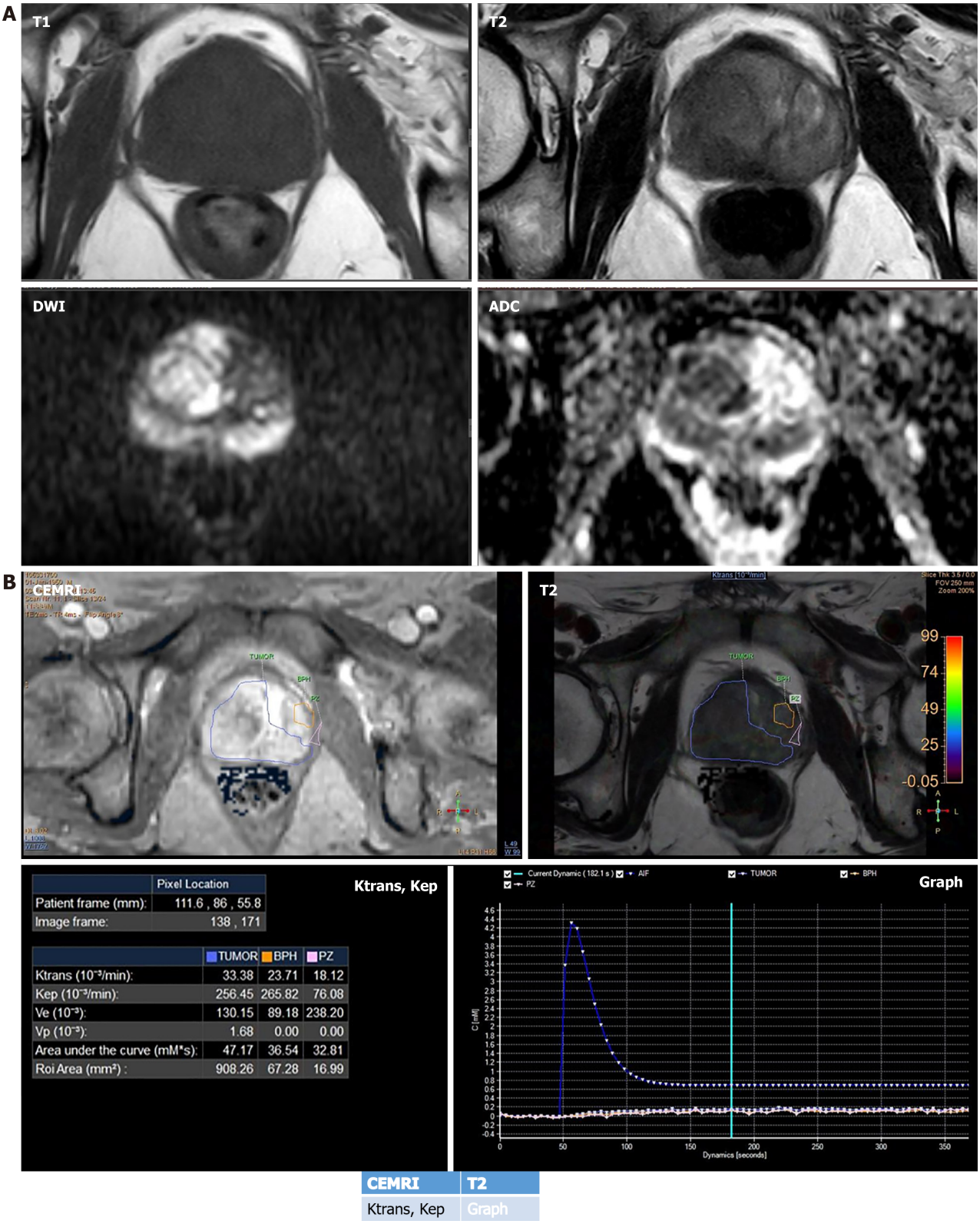

Figure 5 Dynamic contrast-enhanced magnetic resonance imaging based parameters. A: Multiphasic magnetic resonance imaging images show PIRAD 5 lesion in right transitional zone, peripheral zone and left peripheral zone (asterisk); B: Dynamic contrast-enhanced magnetic resonance imaging images show various quantitative parameters. Region of interest has been drawn depicting prostatic cancer and benign prostatic hyperplasia (BPH) nodule. The table in B demonstrates higher Ktrans and Ve value in the prostatic cancer region as compared to BPH nodule. While Kep value is lower in the prostatic cancer region as compared to BPH nodule. The qualitative signal intensity curve in B demonstrates rapid wash in (steeper slope) and fast wash out in prostatic cancer region which is the characteristic curve for malignant tumors.

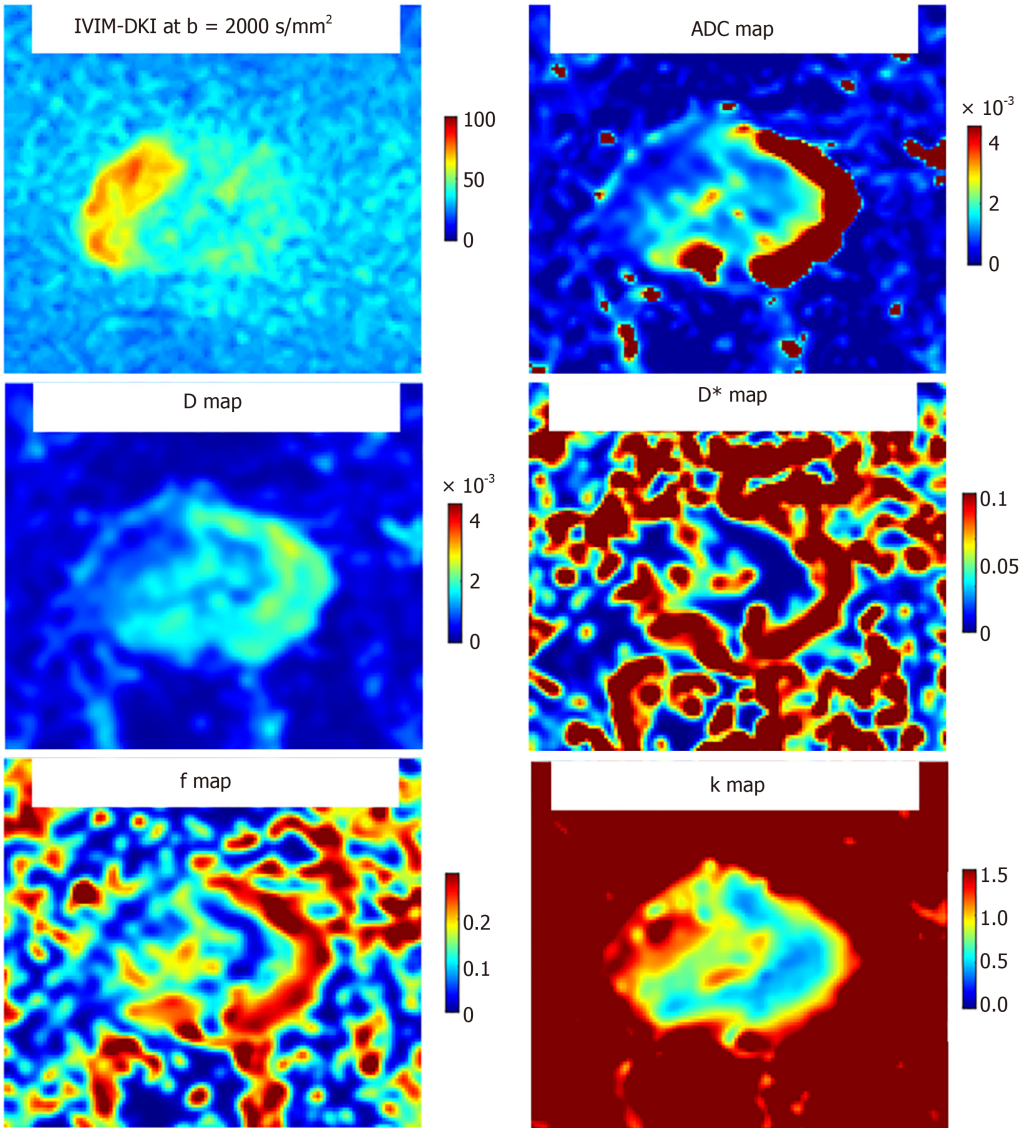

Figure 6 Intravoxel incoherent motion: Intravoxel incoherent motion-diffusion kurtosis imaging at *b* value 2000 second/mm² showing apparent diffusion coefficient map, D map, D* map, f map and k map. The prostatic cancer region is hyperintense in the background of hypointense gland on *b* 2000 second/mm² image and hypointense on apparent diffusion coefficient image.

103]. Thus, there is a controversy as to whether IVIM adds some value over and above ADC or not as there are studies that have found no added role of IVIM over ADC[104].

T1 relaxometry and MR fingerprinting

T1 relaxometry is a potential quantitative technique that enables the assessment of tissue properties by measuring the T1 relaxation time. T1 relaxation is an intrinsic property of any specific tissue and it is defined as the time taken by the longitudinal magnetization to recover 66.6% of its initial value[105]. Conventional sequences can quantify either T1 or T2 relaxation at one time, while the recently introduced MR fingerprinting technique enables quick and concomitant production of quantitative maps of different tissue properties including T1 and T2 relaxation time[106-109]. This technique is based on the pseudorandom variation of MRI properties like repetition time and flip angle so that unique signals are generated for each combination of tissue properties and then a chain of all possible signal evolutions is calculated for that particular sequence[110]. So far, multiple studies have been carried out to verify the role of T2 relaxation time[108,109]. In a recent study including 104 PZ cases, it was found that a combination of T1, T2 relaxometry, and ADC mapping could be useful for quantitative analysis of PCa grades and distinguishing it from benign lesions on T2-weighted images[110].

In comparison to T2 relaxometry, T1 relaxometry is relatively less studied in TZ and PZ lesions. It could be specifically more useful in differentiating prostatitis from PCa in TZ, as these both share a similar appearance on T2 images[111]. In one such study by Panda *et al*[111] in TZ lesions, the best results were shown by the combination of T1 and ADC in distinguishing benign and malignant lesions (AUC = 0.94) as well as in discriminating CsPCa from non-CsPCa (AUC = 0.81). ADC value lower than 0.70 × 10^{-3} mm²/second was highly sensitive and a T1 value lower than 1510 ms was found to be more specific for distinguishing benign and malignant lesions. There was an overlap of T2 values between the groups as

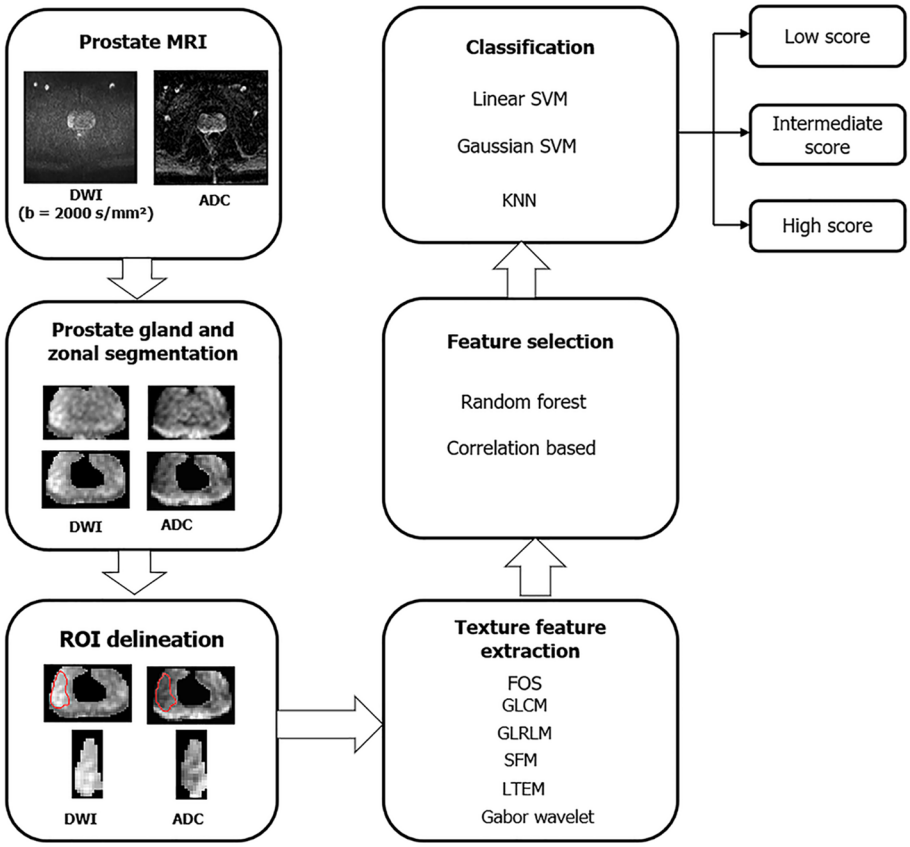

Figure 7 Overview of the framework for texture analysis. MRI: Magnetic resonance imaging; ADC: Apparent diffusion coefficient; DWI: Diffusion-weighted imaging; FOS: First-order statistics; GLCM: Grey level co-occurrence matrix; GLRLM: Grey level run length matrix; KNN: K-nearest neighbor; LTEM: Laws texture energy measures; ROI: Region of interest; SFM: Statistical feature matrix; SVM: Support vector machine.

expected. A study by Yu *et al*[112] in 2017 was the first one in the literature to study T1 differences between benign and malignant PZ lesions. In their study, T1 was significantly less in PZ Ca as compared to adjacent normal PZ. They also pointed out that the history of recent biopsy should always be elicited from the patient, as post-biopsy haemorrhage itself shortens the T1 time, resulting in fallacious results. However, the role of T1 relaxometry in PZ lesions still needs validation by larger studies.

TA

Tumour heterogeneity plays an important role in predicting a tumour's aggressiveness. TA is a statistical tool to measure this tumor heterogeneity through a complex analysis of the spatial distribution of image pixels, grossly not recognizable on conventional sequences[113] (overview of framework for TA shown in Figure 7). Thus, TA could become a non-invasive imaging biomarker for PCa diagnosis, prognosis, and follow-up. The most widely used and verified technique of quantitative TA is the filtration-histogram technique[114]. First-order TA features are based on the extraction of pixel intensity values within a specific area of interest. Second-order statistics measure the association between two pixels while higher-order TA analyses the association among more than two pixels. Some of the texture features which are most widely studied and commonly employed in PCa are entropy (represents histogram's randomness) and kurtosis (represents histogram's peakedness/flatness)[115]. A recent study suggested that after applying the filtration technique, a medium texture scale (3-5 mm) is better to assess tumoral heterogeneity compared to a fine texture scale (2 mm)[116]. A study by Wibmer *et al*[117] showed that ADC-derived higher entropy values (P = 0.0069) and lower energy values (P = 0.0039) showed good correlation with GS, but there was no association of T2-based texture features with GS. Association between any specific texture feature and GS was studied by Baek *et al*[118] using bi-parametric MRI. They found that ADC-derived grey level co-occurrence matrix entropy was associated with GS in patients with PCa, with moderately good (82%) accuracy for discriminating CsPCa from non-CsPCa. Significant association between ADC entropy and PCa aggressiveness has also been shown by studies, with improved sensitivity for ECE detection compared to subjective analysis[119]. A recent study compared ADC-derived texture features and T2-derived texture features[120]. They found that the combination of three ADC texture features *i.e.*, skewness, kurtosis, and entropy predicted high-grade PCa. Texture features of combined IVIM-DKI parameters showed high accuracy and AUC in PCa detection[100]. All these above-mentioned studies bring us to conclude that texture features based on the ADC map have proven to be better in PCa diagnosis and risk stratification. T2-weighted textural features correlation with GS has varied among various studies, few studies have found a correlation while others have not[117,120]. TA can also better detect intraductal carcinoma which usually remains undetected on conventional MRI sequences[121].

Magnetic resonance elastography

Magnetic resonance elastography (MRE) is a non-invasive method that uses low-frequency vibrations to quantitatively measure tissue elasticity and stiffness. In comparison to other quantitative MR techniques, it has the potential to overcome the common limitation of all techniques *i.e.*, inter-observer variability. In a prospective study by Li *et al*[122] involving 73 patients, stiffness and fluidity quantification using tomoelastography improved the diagnostic yield of multiparametric MRI in detecting PCa in both PZ and TZ. Pre-operative MRE-based PCa stiffness measurement can even help in predicting the degree of lymph node metastasis, with sensitivity and specificity as high as 100% and 86.5%, respectively[123].

MRE is a non-invasive method that uses low-frequency vibrations to quantitatively measure tissue elasticity and stiffness. In comparison to other quantitative MR techniques, it has the potential to overcome the common limitation of all techniques *i.e.*, inter-observer variability. In a prospective study by Li *et al*[122] involving 73 patients, stiffness and fluidity quantification using tomoelastography improved the diagnostic yield of multiparametric MRI in detecting PCa in both PZ and TZ. Pre-operative MRE-based PCa stiffness measurement can even help in predicting the degree of lymph node metastasis, with sensitivity and specificity as high as 100% and 86.5%, respectively[123].

CONCLUSION

Quantitative imaging has many advantages over conventional qualitative assessment. A few parameters have also been shown to correlate with the GS and can help in deciding disease prognosis and clinical management. Many such MRI based quantitative imaging metrics have been discussed thoroughly in this article. Few of these are already part of PIRADS, while many are under study and can be incorporated into clinical practice in the future after validation by rigorous multicentre studies. One major hurdle in achieving the quantification is the fact that numerical values obtained tend to differ from center to center because of many factors including differences in scanners, individual imaging protocols, and techniques, *etc.* The applications of features like TV and size, LCC, ADC values need a standardized cut off values to achieve their full clinical potential. An ideal metric would be one that is easy to calculate, and less prone to errors because of differences in scanners, individual imaging protocols, and techniques. A quantitative imaging marker could improve PCa detection by minimizing inter-radiologist subjectivity, thereby reducing overdiagnosis. This would help avoid unnecessary biopsies and decrease the overtreatment of slow-growing PCa.

FOOTNOTES

Author contributions: Dhiman A, Kumar V, and Das CJ wrote the manuscript; Kumar V and Das CJ supervised and finally approval of the manuscript.

Conflict-of-interest statement: All the authors report no relevant conflicts of interest for this article.

Country of origin: India

ORCID number: Chandan Jyoti Das 0000-0001-6505-5940.

S-Editor: Wang JJ
L-Editor: A
P-Editor: Yu HG

REFERENCES

1 **Bray F**, Laversanne M, Sung H, Ferlay J, Siegel RL, Soerjomataram I, Jemal A. Global cancer statistics 2022: GLOBOCAN estimates of incidence and mortality worldwide for 36 cancers in 185 countries. *CA Cancer J Clin* 2024; **74**: 229-263 [PMID: 38572751 DOI: 10.3322/caac.21834]

2 **Reddy RR**, Jagannathan NR. Potential of nuclear magnetic resonance metabolomics in the study of prostate cancer. *Indian J Urol* 2022; **38**: 99-109 [PMID: 35400867 DOI: 10.4103/iju.iju_416_21]

3 **Fernandes MC**, Yildirim O, Woo S, Vargas HA, Hricak H. The role of MRI in prostate cancer: current and future directions. *MAGMA* 2022; **35**: 503-521 [PMID: 35294642 DOI: 10.1007/s10334-022-01006-6]

4 **Rebello RJ**, Oing C, Knudsen KE, Loeb S, Johnson DC, Reiter RE, Gillessen S, Van der Kwast T, Bristow RG. Prostate cancer. *Nat Rev Dis Primers* 2021; **7**: 9 [PMID: 33542230 DOI: 10.1038/s41572-020-00243-0]

5 **Lucarelli NM**, Villanova I, Maggialetti N, Greco S, Tarantino F, Russo R, Trabucco SMR, Stabile Ianora AA, Scardapane A. Quantitative ADC: An Additional Tool in the Evaluation of Prostate Cancer? *J Pers Med* 2023; **13** [PMID: 37763146 DOI: 10.3390/jpm13091378]

6 **Turkbey B**, Rosenkrantz AB, Haider MA, Padhani AR, Villeirs G, Macura KJ, Tempany CM, Choyke PL, Cornud F, Margolis DJ, Thoeny HC, Verma S, Barentsz J, Weinreb JC. Prostate Imaging Reporting and Data System Version 2.1: 2019 Update of Prostate Imaging Reporting and Data System Version 2. *Eur Urol* 2019; **76**: 340-351 [PMID: 30898406 DOI: 10.1016/j.eururo.2019.02.033]

7 **Qayyum A**. Diffusion-weighted imaging in the abdomen and pelvis: concepts and applications. *Radiographics* 2009; **29**: 1797-1810 [PMID: 19959522 DOI: 10.1148/rg.296095521]

8 **Thoeny HC**, De Keyzer F. Extracranial applications of diffusion-weighted magnetic resonance imaging. *Eur Radiol* 2007; **17**: 1385-1393 [PMID: 17206421 DOI: 10.1007/s00330-006-0547-0]

9 **Kumar V**, Jagannathan NR, Kumar R, Das SC, Jindal L, Thulkar S, Gupta SD, Dwivedi SN, Roell S, Hemal AK, Gupta NP. Correlation between metabolite ratios and ADC values of prostate in men with increased PSA level. *Magn Reson Imaging* 2006; **24**: 541-548 [PMID: 16735174 DOI: 10.1016/j.mri.2006.01.001]

10 **Kumar V**, Jagannathan NR, Kumar R, Thulkar S, Gupta SD, Dwivedi SN, Hemal AK, Gupta NP. Apparent diffusion coefficient of the prostate in men prior to biopsy: determination of a cut-off value to predict malignancy of the peripheral zone. *NMR Biomed* 2007; **20**: 505-511 [PMID: 17167820 DOI: 10.1002/nbm.1114]

11 **Rosenkrantz AB**, Parikh N, Kierans AS, Kong MX, Babb JS, Taneja SS, Ream JM. Prostate Cancer Detection Using Computed Very High b-value Diffusion-weighted Imaging: How High Should We Go? *Acad Radiol* 2016; **23**: 704-711 [PMID: 26992738 DOI: 10.1016/j.acra.2016.02.003]

12 **Rosenkrantz AB**, Hindman N, Lim RP, Das K, Babb JS, Mussi TC, Taneja SS. Diffusion-weighted imaging of the prostate: Comparison of b1000 and b2000 image sets for index lesion detection. *J Magn Reson Imaging* 2013; **38**: 694-700 [PMID: 23371846 DOI: 10.1002/jmri.24016]

13 **Ueno Y**, Kitajima K, Sugimura K, Kawakami F, Miyake H, Obara M, Takahashi S. Ultra-high b-value diffusion-weighted MRI for the detection of prostate cancer with 3-T MRI. *J Magn Reson Imaging* 2013; **38**: 154-160 [PMID: 23292979 DOI: 10.1002/jmri.23953]

14 **Wang X**, Qian Y, Liu B, Cao L, Fan Y, Zhang JJ, Yu Y. High-b-value diffusion-weighted MRI for the detection of prostate cancer at 3 T. *Clin Radiol* 2014; **69**: 1165-1170 [PMID: 25182363 DOI: 10.1016/j.crad.2014.07.013]

15 **Wetter A**, Nensa F, Lipponer C, Guberina N, Olbricht T, Schenck M, Schlosser TW, Gratz M, Lauenstein TC. High and ultra-high b-value diffusion-weighted imaging in prostate cancer: a quantitative analysis. *Acta Radiol* 2015; **56**: 1009-1015 [PMID: 25168023 DOI: 10.1177/0284185114547900]

16 **Metens T**, Miranda D, Absil J, Matos C. What is the optimal b value in diffusion-weighted MR imaging to depict prostate cancer at 3T? *Eur Radiol* 2012; **22**: 703-709 [PMID: 21971824 DOI: 10.1007/s00330-011-2298-9]

17 **Agarwal HK**, Mertan FV, Sankineni S, Bernardo M, Senegas J, Keupp J, Daar D, Merino M, Wood BJ, Pinto PA, Choyke PL, Turkbey B. Optimal high b-value for diffusion weighted MRI in diagnosing high risk prostate cancers in the peripheral zone. *J Magn Reson Imaging* 2017; **45**: 125-131 [PMID: 27383502 DOI: 10.1002/jmri.25353]

18 **Ohgiya Y**, Suyama J, Seino N, Hashizume T, Kawahara M, Sai S, Saiki M, Munechika J, Hirose M, Gokan T. Diagnostic accuracy of ultra-high-b-value 3.0-T diffusion-weighted MR imaging for detection of prostate cancer. *Clin Imaging* 2012; **36**: 526-531 [PMID: 22920357 DOI: 10.1016/j.clinimag.2011.11.016]

19 **Rosenkrantz AB**, Chandarana H, Hindman N, Deng FM, Babb JS, Taneja SS, Geppert C. Computed diffusion-weighted imaging of the prostate at 3 T: impact on image quality and tumour detection. *Eur Radiol* 2013; **23**: 3170-3177 [PMID: 23756956 DOI: 10.1007/s00330-013-2917-8]

20 **Kwon MR**, Kim CK, Kim JH. PI-RADS version 2: evaluation of diffusion-weighted imaging interpretation between b = 1000 and b = 1500 s mm(-)(2). *Br J Radiol* 2017; **90**: 20170438 [PMID: 28830221 DOI: 10.1259/bjr.20170438]

21 **Rosenkrantz AB**, Padhani AR, Chenevert TL, Koh DM, De Keyzer F, Taouli B, Le Bihan D. Body diffusion kurtosis imaging: Basic principles, applications, and considerations for clinical practice. *J Magn Reson Imaging* 2015; **42**: 1190-1202 [PMID: 26119267 DOI: 10.1002/jmri.24985]

22 **Weinreb JC**, Barentsz JO, Choyke PL, Cornud F, Haider MA, Macura KJ, Margolis D, Schnall MD, Shtern F, Tempany CM, Thoeny HC, Verma S. PI-RADS Prostate Imaging - Reporting and Data System: 2015, Version 2. *Eur Urol* 2016; **69**: 16-40 [PMID: 26427566 DOI: 10.1016/j.eururo.2015.08.052]

23 **Verma S**, Rajesh A, Morales H, Lemen L, Bills G, Delworth M, Gaitonde K, Ying J, Samartunga R, Lamba M. Assessment of aggressiveness of prostate cancer: correlation of apparent diffusion coefficient with histologic grade after radical prostatectomy. *AJR Am J Roentgenol* 2011; **196**: 374-381 [PMID: 21257890 DOI: 10.2214/AJR.10.4441]

24 **Woodfield CA**, Tung GA, Grand DJ, Pezzullo JA, Machan JT, Renzulli JF 2nd. Diffusion-weighted MRI of peripheral zone prostate cancer: comparison of tumor apparent diffusion coefficient with Gleason score and percentage of tumor on core biopsy. *AJR Am J Roentgenol* 2010; **194**: W316-W322 [PMID: 20308476 DOI: 10.2214/AJR.09.2651]

25 **Vargas HA**, Akin O, Franiel T, Mazaheri Y, Zheng J, Moskowitz C, Udo K, Eastham J, Hricak H. Diffusion-weighted endorectal MR imaging at 3 T for prostate cancer: tumor detection and assessment of aggressiveness. *Radiology* 2011; **259**: 775-784 [PMID: 21436085 DOI: 10.1148/radiol.11102066]

26 **Donati OF**, Mazaheri Y, Afaq A, Vargas HA, Zheng J, Moskowitz CS, Hricak H, Akin O. Prostate cancer aggressiveness: assessment with whole-lesion histogram analysis of the apparent diffusion coefficient. *Radiology* 2014; **271**: 143-152 [PMID: 24475824 DOI: 10.1148/radiol.13130973]

27 **Tamada T**, Prabhu V, Li J, Babb JS, Taneja SS, Rosenkrantz AB. Assessment of prostate cancer aggressiveness using apparent diffusion coefficient values: impact of patient race and age. *Abdom Radiol (NY)* 2017; **42**: 1744-1751 [PMID: 28161826 DOI: 10.1007/s00261-017-1058-y]

28 **Litjens GJ**, Hambrock T, Hulsbergen-van de Kaa C, Barentsz JO, Huisman HJ. Interpatient variation in normal peripheral zone apparent diffusion coefficient: effect on the prediction of prostate cancer aggressiveness. *Radiology* 2012; **265**: 260-266 [PMID: 22923722 DOI: 10.1148/radiol.12112374]

29 **Chatterjee A**, Gallan AJ, He D, Fan X, Mustafi D, Yousuf A, Antic T, Karczmar GS, Oto A. Revisiting quantitative multi-parametric MRI of benign prostatic hyperplasia and its differentiation from transition zone cancer. *Abdom Radiol (NY)* 2019; **44**: 2233-2243 [PMID: 30955071 DOI: 10.1007/s00261-019-01936-1]

30 **Kitzing YX**, Prando A, Varol C, Karczmar GS, Maclean F, Oto A. Benign Conditions That Mimic Prostate Carcinoma: MR Imaging Features with Histopathologic Correlation. *Radiographics* 2016; **36**: 162-175 [PMID: 26587887 DOI: 10.1148/rg.2016150030]

31 **Woo S**, Kim SY, Cho JY, Kim SH. Preoperative Evaluation of Prostate Cancer Aggressiveness: Using ADC and ADC Ratio in Determining

Gleason Score. *AJR Am J Roentgenol* 2016; **207**: 114-120 [PMID: 27077643 DOI: 10.2214/AJR.15.15894]
32 **Rosenkrantz AB**, Kopec M, Kong X, Melamed J, Dakwar G, Babb JS, Taouli B. Prostate cancer vs. post-biopsy hemorrhage: diagnosis with T2- and diffusion-weighted imaging. *J Magn Reson Imaging* 2010; **31**: 1387-1394 [PMID: 20512891 DOI: 10.1002/jmri.22172]
33 **Bajgiran AM**, Mirak SA, Sung K, Sisk AE, Reiter RE, Raman SS. Apparent Diffusion Coefficient (ADC) Ratio Versus Conventional ADC for Detecting Clinically Significant Prostate Cancer With 3-T MRI. *AJR Am J Roentgenol* 2019; **213**: W134-W142 [PMID: 31216201 DOI: 10.2214/AJR.19.21365]
34 **Giganti F**, Pecoraro M, Fierro D, Campa R, Del Giudice F, Punwani S, Kirkham A, Allen C, Emberton M, Catalano C, Moore CM, Panebianco V. DWI and PRECISE criteria in men on active surveillance for prostate cancer: A multicentre preliminary experience of different ADC calculations. *Magn Reson Imaging* 2020; **67**: 50-58 [PMID: 31899283 DOI: 10.1016/j.mri.2019.12.007]
35 **Fennessy FM**, Maier SE. Quantitative diffusion MRI in prostate cancer: Image quality, what we can measure and how it improves clinical assessment. *Eur J Radiol* 2023; **167**: 111066 [PMID: 37651828 DOI: 10.1016/j.ejrad.2023.111066]
36 **Jyoti R**, Jain TP, Haxhimolla H, Liddell H, Barrett SE. Correlation of apparent diffusion coefficient ratio on 3.0 T MRI with prostate cancer Gleason score. *Eur J Radiol Open* 2018; **5**: 58-63 [PMID: 29687050 DOI: 10.1016/j.ejro.2018.03.002]
37 **Barrett T**, Priest AN, Lawrence EM, Goldman DA, Warren AY, Gnanapragasam VJ, Sala E, Gallagher FA. Ratio of Tumor to Normal Prostate Tissue Apparent Diffusion Coefficient as a Method for Quantifying DWI of the Prostate. *AJR Am J Roentgenol* 2015; **205**: W585-W593 [PMID: 26587948 DOI: 10.2214/AJR.15.14338]
38 **De Cobelli F**, Ravelli S, Esposito A, Giganti F, Gallina A, Montorsi F, Del Maschio A. Apparent diffusion coefficient value and ratio as noninvasive potential biomarkers to predict prostate cancer grading: comparison with prostate biopsy and radical prostatectomy specimen. *AJR Am J Roentgenol* 2015; **204**: 550-557 [PMID: 25714284 DOI: 10.2214/AJR.14.13146]
39 **Rozenberg R**, Thornhill RE, Flood TA, Hakim SW, Lim C, Schieda N. Whole-Tumor Quantitative Apparent Diffusion Coefficient Histogram and Texture Analysis to Predict Gleason Score Upgrading in Intermediate-Risk 3 + 4 = 7 Prostate Cancer. *AJR Am J Roentgenol* 2016; **206**: 775-782 [PMID: 27003049 DOI: 10.2214/AJR.15.15462]
40 **Wu X**, Reinikainen P, Vanhanen A, Kapanen M, Vierikko T, Ryymin P, Hyödynmaa S, Kellokumpu-Lehtinen PL. Correlation between apparent diffusion coefficient value on diffusion-weighted MR imaging and Gleason score in prostate cancer. *Diagn Interv Imaging* 2017; **98**: 63-71 [PMID: 27687831 DOI: 10.1016/j.diii.2016.08.009]
41 **Zhang Z**, Xu H, Xue Y, Li J, Ye Q. Risk Stratification of Prostate Cancer Using the Combination of Histogram Analysis of Apparent Diffusion Coefficient Across Tumor Diffusion Volume and Clinical Information: A Pilot Study. *J Magn Reson Imaging* 2019; **49**: 556-564 [PMID: 30173421 DOI: 10.1002/jmri.26235]
42 **Surov A**, Meyer HJ, Wienke A. Correlations between Apparent Diffusion Coefficient and Gleason Score in Prostate Cancer: A Systematic Review. *Eur Urol Oncol* 2020; **3**: 489-497 [PMID: 31412009 DOI: 10.1016/j.euo.2018.12.006]
43 **Priester A**, Natarajan S, Khoshnoodi P, Margolis DJ, Raman SS, Reiter RE, Huang J, Grundfest W, Marks LS. Magnetic Resonance Imaging Underestimation of Prostate Cancer Geometry: Use of Patient Specific Molds to Correlate Images with Whole Mount Pathology. *J Urol* 2017; **197**: 320-326 [PMID: 27484386 DOI: 10.1016/j.juro.2016.07.084]
44 **Stamey TA**, McNeal JE, Freiha FS, Redwine E. Morphometric and clinical studies on 68 consecutive radical prostatectomies. *J Urol* 1988; **139**: 1235-1241 [PMID: 3373594 DOI: 10.1016/s0022-5347(17)42876-x]
45 **Knoedler JJ**, Karnes RJ, Thompson RH, Rangel LJ, Bergstralh EJ, Boorjian SA. The association of tumor volume with mortality following radical prostatectomy. *Prostate Cancer Prostatic Dis* 2014; **17**: 144-148 [PMID: 24469091 DOI: 10.1038/pcan.2013.61]
46 **Egevad L**, Norberg M, Mattson S, Norlén BJ, Busch C. Estimation of prostate cancer volume by multiple core biopsies before radical prostatectomy. *Urology* 1998; **52**: 653-658 [PMID: 9763088 DOI: 10.1016/s0090-4295(98)00221-0]
47 **Muller BG**, Fütterer JJ, Gupta RT, Katz A, Kirkham A, Kurhanewicz J, Moul JW, Pinto PA, Rastinehad AR, Robertson C, de la Rosette J, Sanchez-Salas R, Jones JS, Ukimura O, Verma S, Wijkstra H, Marberger M. The role of magnetic resonance imaging (MRI) in focal therapy for prostate cancer: recommendations from a consensus panel. *BJU Int* 2014; **113**: 218-227 [PMID: 24215670 DOI: 10.1111/bju.12243]
48 **Moore CM**, Giganti F, Albertsen P, Allen C, Bangma C, Briganti A, Carroll P, Haider M, Kasivisvanathan V, Kirkham A, Klotz L, Ouzzane A, Padhani AR, Panebianco V, Pinto P, Puech P, Rannikko A, Renard-Penna R, Touijer K, Turkbey B, van Poppel H, Valdagni R, Walz J, Schoots I. Reporting Magnetic Resonance Imaging in Men on Active Surveillance for Prostate Cancer: The PRECISE Recommendations-A Report of a European School of Oncology Task Force. *Eur Urol* 2017; **71**: 648-655 [PMID: 27349615 DOI: 10.1016/j.eururo.2016.06.011]
49 **Gholami N**, Haghparast A, Alipourfard I, Nazari M. Prostate cancer in omics era. *Cancer Cell Int* 2022; **22**: 274 [PMID: 36064406 DOI: 10.1186/s12935-022-02691-y]
50 **Mazzucchelli R**, Scarpelli M, Cheng L, Lopez-Beltran A, Galosi AB, Kirkali Z, Montironi R. Pathology of prostate cancer and focal therapy ('male lumpectomy'). *Anticancer Res* 2009; **29**: 5155-5161 [PMID: 20044631]
51 **Lindner U**, Lawrentschuk N, Trachtenberg J. Image guidance for focal therapy of prostate cancer. *World J Urol* 2010; **28**: 727-734 [PMID: 20963422 DOI: 10.1007/s00345-010-0604-9]
52 **McNeal JE**, Villers AA, Redwine EA, Freiha FS, Stamey TA. Capsular penetration in prostate cancer. Significance for natural history and treatment. *Am J Surg Pathol* 1990; **14**: 240-247 [PMID: 2305930 DOI: 10.1097/00000478-199003000-00005]
53 **Villers AA**, McNeal JE, Redwine EA, Freiha FS, Stamey TA. Pathogenesis and biological significance of seminal vesicle invasion in prostatic adenocarcinoma. *J Urol* 1990; **143**: 1183-1187 [PMID: 2342179 DOI: 10.1016/s0022-5347(17)40220-5]
54 **McNeal JE**, Villers AA, Redwine EA, Freiha FS, Stamey TA. Histologic differentiation, cancer volume, and pelvic lymph node metastasis in adenocarcinoma of the prostate. *Cancer* 1990; **66**: 1225-1233 [PMID: 2400973 DOI: 10.1002/1097-0142(19900915)66:6<1225::aid-cncr2820660624>3.0.co;2-x]
55 **Bostwick DG**, Graham SD Jr, Napalkov P, Abrahamsson PA, di Sant'agnese PA, Algaba F, Hoisaeter PA, Lee F, Littrup P, Mostofi FK. Staging of early prostate cancer: a proposed tumor volume-based prognostic index. *Urology* 1993; **41**: 403-411 [PMID: 8488608 DOI: 10.1016/0090-4295(93)90497-x]
56 **Hambrock T**, Somford DM, Huisman HJ, van Oort IM, Witjes JA, Hulsbergen-van de Kaa CA, Scheenen T, Barentsz JO. Relationship between apparent diffusion coefficients at 3.0-T MR imaging and Gleason grade in peripheral zone prostate cancer. *Radiology* 2011; **259**: 453-461 [PMID: 21502392 DOI: 10.1148/radiol.11091409]
57 **Mazaheri Y**, Hricak H, Fine SW, Akin O, Shukla-Dave A, Ishill NM, Moskowitz CS, Grater JE, Reuter VE, Zakian KL, Touijer KA, Koutcher JA. Prostate tumor volume measurement with combined T2-weighted imaging and diffusion-weighted MR: correlation with pathologic tumor volume. *Radiology* 2009; **252**: 449-457 [PMID: 19703883 DOI: 10.1148/radiol.2523081423]

58 **Singh D**, Das CJ, Kumar V, Singh A, Mehndiratta A. Quantification of prostate tumour diameter and volume from MR images using 3D ellipsoid model and its impact on PI-RADS v2.1 assessment. *Sci Rep* 2022; **12**: 21501 [PMID: 36513800 DOI: 10.1038/s41598-022-26065-6]

59 **Lovegrove CE**, Matanhelia M, Randeva J, Eldred-Evans D, Tam H, Miah S, Winkler M, Ahmed HU, Shah TT. Prostate imaging features that indicate benign or malignant pathology on biopsy. *Transl Androl Urol* 2018; **7**: S420-S435 [PMID: 30363462 DOI: 10.21037/tau.2018.07.06]

60 **Barentsz JO**, Weinreb JC, Verma S, Thoeny HC, Tempany CM, Shtern F, Padhani AR, Margolis D, Macura KJ, Haider MA, Cornud F, Choyke PL. Synopsis of the PI-RADS v2 Guidelines for Multiparametric Prostate Magnetic Resonance Imaging and Recommendations for Use. *Eur Urol* 2016; **69**: 41-49 [PMID: 26361169 DOI: 10.1016/j.eururo.2015.08.038]

61 **Moosavi B**, Flood TA, Al-Dandan O, Breau RH, Cagiannos I, Morash C, Malone SC, Schieda N. Multiparametric MRI of the anterior prostate gland: clinical-radiological-histopathological correlation. *Clin Radiol* 2016; **71**: 405-417 [PMID: 26888762 DOI: 10.1016/j.crad.2016.01.002]

62 **Shaish H**, Taneja SS, Rosenkrantz AB. Prostate MR Imaging: An Update. *Radiol Clin North Am* 2017; **55**: 303-320 [PMID: 28126217 DOI: 10.1016/j.rcl.2016.10.011]

63 **Li Q**, Lu H, Choi J, Gage K, Feuerlein S, Pow-Sang JM, Gillies R, Balagurunathan Y. Radiological semantics discriminate clinically significant grade prostate cancer. *Cancer Imaging* 2019; **19**: 81 [PMID: 31796094 DOI: 10.1186/s40644-019-0272-y]

64 **Abreu-Gomez J**, Wu M, McInnes MDF, Thornhill RE, Flood TA, Schieda N. Shape Analysis of Peripheral Zone Observations on Prostate DWI: Correlation to Histopathology Outcomes After Radical Prostatectomy. *AJR Am J Roentgenol* 2020; **214**: 1239-1247 [PMID: 32228325 DOI: 10.2214/AJR.19.22318]

65 **Krishna S**, Schieda N, McInnes MD, Flood TA, Thornhill RE. Diagnosis of transition zone prostate cancer using T2-weighted (T2W) MRI: comparison of subjective features and quantitative shape analysis. *Eur Radiol* 2019; **29**: 1133-1143 [PMID: 30105411 DOI: 10.1007/s00330-018-5664-z]

66 **Cuocolo R**, Stanzione A, Ponsiglione A, Romeo V, Verde F, Creta M, La Rocca R, Longo N, Pace L, Imbriaco M. Clinically significant prostate cancer detection on MRI: A radiomic shape features study. *Eur J Radiol* 2019; **116**: 144-149 [PMID: 31153556 DOI: 10.1016/j.ejrad.2019.05.006]

67 **Baco E**, Rud E, Vlatkovic L, Svindland A, Eggesbø HB, Hung AJ, Matsugasumi T, Bernhard JC, Gill IS, Ukimura O. Predictive value of magnetic resonance imaging determined tumor contact length for extracapsular extension of prostate cancer. *J Urol* 2015; **193**: 466-472 [PMID: 25150643 DOI: 10.1016/j.juro.2014.08.084]

68 **Wibmer A**, Vargas HA, Donahue TF, Zheng J, Moskowitz C, Eastham J, Sala E, Hricak H. Diagnosis of Extracapsular Extension of Prostate Cancer on Prostate MRI: Impact of Second-Opinion Readings by Subspecialized Genitourinary Oncologic Radiologists. *AJR Am J Roentgenol* 2015; **205**: W73-W78 [PMID: 26102421 DOI: 10.2214/AJR.14.13600]

69 **de Rooij M**, Hamoen EH, Witjes JA, Barentsz JO, Rovers MM. Accuracy of Magnetic Resonance Imaging for Local Staging of Prostate Cancer: A Diagnostic Meta-analysis. *Eur Urol* 2016; **70**: 233-245 [PMID: 26215604 DOI: 10.1016/j.eururo.2015.07.029]

70 **Fütterer JJ**, Engelbrecht MR, Jager GJ, Hartman RP, King BF, Hulsbergen-Van de Kaa CA, Witjes JA, Barentsz JO. Prostate cancer: comparison of local staging accuracy of pelvic phased-array coil alone versus integrated endorectal-pelvic phased-array coils. Local staging accuracy of prostate cancer using endorectal coil MR imaging. *Eur Radiol* 2007; **17**: 1055-1065 [PMID: 17024497 DOI: 10.1007/s00330-006-0418-8]

71 **Onay A**, Vural M, Armutlu A, Ozel Yıldız S, Kiremit MC, Esen T, Bakır B. Evaluation of the most optimal multiparametric magnetic resonance imaging sequence for determining pathological length of capsular contact. *Eur J Radiol* 2019; **112**: 192-199 [PMID: 30777210 DOI: 10.1016/j.ejrad.2019.01.020]

72 **Rosenkrantz AB**, Shanbhogue AK, Wang A, Kong MX, Babb JS, Taneja SS. Length of capsular contact for diagnosing extraprostatic extension on prostate MRI: Assessment at an optimal threshold. *J Magn Reson Imaging* 2016; **43**: 990-997 [PMID: 26395278 DOI: 10.1002/jmri.25040]

73 **Woo S**, Kim SY, Cho JY, Kim SH. Length of capsular contact on prostate MRI as a predictor of extracapsular extension: which is the most optimal sequence? *Acta Radiol* 2017; **58**: 489-497 [PMID: 27439401 DOI: 10.1177/0284185116658684]

74 **Kim TH**, Woo S, Han S, Suh CH, Ghafoor S, Hricak H, Vargas HA. The Diagnostic Performance of the Length of Tumor Capsular Contact on MRI for Detecting Prostate Cancer Extraprostatic Extension: A Systematic Review and Meta-Analysis. *Korean J Radiol* 2020; **21**: 684-694 [PMID: 32410407 DOI: 10.3348/kjr.2019.0842]

75 **Kongnyuy M**, Sidana A, George AK, Muthigi A, Iyer A, Ho R, Chelluri R, Mertan F, Frye TP, Su D, Merino MJ, Choyke PL, Wood BJ, Pinto PA, Turkbey B. Tumor contact with prostate capsule on magnetic resonance imaging: A potential biomarker for staging and prognosis. *Urol Oncol* 2017; **35**: 30.e1-30.e8 [PMID: 27567248 DOI: 10.1016/j.urolonc.2016.07.013]

76 **Granja MF**, Pedraza CM, Flórez DC, Romero JA, Palau MA, Aguirre DA. Predicting extracapsular involvement in prostate cancer through the tumor contact length and the apparent diffusion coefficient. *Radiologia* 2017; **59**: 313-320 [PMID: 28473218 DOI: 10.1016/j.rx.2017.03.003]

77 **Lawrence EM**, Gallagher FA, Barrett T, Warren AY, Priest AN, Goldman DA, Sala E, Gnanapragasam VJ. Preoperative 3-T diffusion-weighted MRI for the qualitative and quantitative assessment of extracapsular extension in patients with intermediate- or high-risk prostate cancer. *AJR Am J Roentgenol* 2014; **203**: W280-W286 [PMID: 25148185 DOI: 10.2214/AJR.13.11754]

78 **Tamada T**, Sone T, Jo Y, Toshimitsu S, Yamashita T, Yamamoto A, Tanimoto D, Ito K. Apparent diffusion coefficient values in peripheral and transition zones of the prostate: comparison between normal and malignant prostatic tissues and correlation with histologic grade. *J Magn Reson Imaging* 2008; **28**: 720-726 [PMID: 18777532 DOI: 10.1002/jmri.21503]

79 **Schlemmer HP**, Merkle J, Grobholz R, Jaeger T, Michel MS, Werner A, Rabe J, van Kaick G. Can pre-operative contrast-enhanced dynamic MR imaging for prostate cancer predict microvessel density in prostatectomy specimens? *Eur Radiol* 2004; **14**: 309-317 [PMID: 14531000 DOI: 10.1007/s00330-003-2025-2]

80 **Kiessling F**, Lichy M, Grobholz R, Heilmann M, Farhan N, Michel MS, Trojan L, Ederle J, Abel U, Kauczor HU, Semmler W, Delorme S. Simple models improve the discrimination of prostate cancers from the peripheral gland by T1-weighted dynamic MRI. *Eur Radiol* 2004; **14**: 1793-1801 [PMID: 15232714 DOI: 10.1007/s00330-004-2386-1]

81 **Franiel T**, Lüdemann L, Rudolph B, Rehbein H, Stephan C, Taupitz M, Beyersdorff D. Prostate MR imaging: tissue characterization with pharmacokinetic volume and blood flow parameters and correlation with histologic parameters. *Radiology* 2009; **252**: 101-108 [PMID: 19561252 DOI: 10.1148/radiol.2521081400]

82 **Verma S**, Turkbey B, Muradyan N, Rajesh A, Cornud F, Haider MA, Choyke PL, Harisinghani M. Overview of dynamic contrast-enhanced MRI in prostate cancer diagnosis and management. *AJR Am J Roentgenol* 2012; **198**: 1277-1288 [PMID: 22623539 DOI: 10.2214/AJR.12.8510]

83 **Vos EK**, Litjens GJ, Kobus T, Hambrock T, Hulsbergen-van de Kaa CA, Barentsz JO, Huisman HJ, Scheenen TW. Assessment of prostate

cancer aggressiveness using dynamic contrast-enhanced magnetic resonance imaging at 3 T. *Eur Urol* 2013; **64**: 448-455 [PMID: 23751135 DOI: 10.1016/j.eururo.2013.05.045]

84 **Rosida YR**, Sukmaningtyas H, Imawati S, Prajoko YW, Sadhana U. Qualitative and quantitative parameters of dynamic contrast-enhanced (DCE) MRI as a diagnostic determinant of soft tissue tumor malignancy: a study from Indonesia. *Egypt J Radiol Nucl Med* 2023; **54**: 118 [DOI: 10.1186/s43055-023-01064-3]

85 **Li C**, Chen M, Li S, Zhao X, Zhang C, Luo X, Zhou C. Detection of prostate cancer in peripheral zone: comparison of MR diffusion tensor imaging, quantitative dynamic contrast-enhanced MRI, and the two techniques combined at 3.0 T. *Acta Radiol* 2014; **55**: 239-247 [PMID: 23892233 DOI: 10.1177/0284185113494978]

86 **Hötker AM**, Mazaheri Y, Aras Ö, Zheng J, Moskowitz CS, Gondo T, Matsumoto K, Hricak H, Akin O. Assessment of Prostate Cancer Aggressiveness by Use of the Combination of Quantitative DWI and Dynamic Contrast-Enhanced MRI. *AJR Am J Roentgenol* 2016; **206**: 756-763 [PMID: 26900904 DOI: 10.2214/AJR.15.14912]

87 **Turkbey B**, Pinto PA, Mani H, Bernardo M, Pang Y, McKinney YL, Khurana K, Ravizzini GC, Albert PS, Merino MJ, Choyke PL. Prostate cancer: value of multiparametric MR imaging at 3 T for detection--histopathologic correlation. *Radiology* 2010; **255**: 89-99 [PMID: 20308447 DOI: 10.1148/radiol.09090475]

88 **Berman RM**, Brown AM, Chang SD, Sankineni S, Kadakia M, Wood BJ, Pinto PA, Choyke PL, Turkbey B. DCE MRI of prostate cancer. *Abdom Radiol (NY)* 2016; **41**: 844-853 [PMID: 27193787 DOI: 10.1007/s00261-015-0589-3]

89 **Oto A**, Yang C, Kayhan A, Tretiakova M, Antic T, Schmid-Tannwald C, Eggener S, Karczmar GS, Stadler WM. Diffusion-weighted and dynamic contrast-enhanced MRI of prostate cancer: correlation of quantitative MR parameters with Gleason score and tumor angiogenesis. *AJR Am J Roentgenol* 2011; **197**: 1382-1390 [PMID: 22109293 DOI: 10.2214/AJR.11.6861]

90 **Feng X**, Chen X, Peng P, Zhou H, Hong Y, Zhu C, Lu L, Xie S, Zhang S, Long L. Values of multiparametric and biparametric MRI in diagnosing clinically significant prostate cancer: a multivariate analysis. *BMC Urol* 2024; **24**: 40 [PMID: 38365673 DOI: 10.1186/s12894-024-01411-0]

91 **Le Bihan D**, Breton E, Lallemand D, Aubin ML, Vignaud J, Laval-Jeantet M. Separation of diffusion and perfusion in intravoxel incoherent motion MR imaging. *Radiology* 1988; **168**: 497-505 [PMID: 3393671 DOI: 10.1148/radiology.168.2.3393671]

92 **Le Bihan D**. Intravoxel incoherent motion perfusion MR imaging: a wake-up call. *Radiology* 2008; **249**: 748-752 [PMID: 19011179 DOI: 10.1148/radiol.2493081301]

93 **Tamura C**, Shinmoto H, Soga S, Okamura T, Sato H, Okuaki T, Pang Y, Kosuda S, Kaji T. Diffusion kurtosis imaging study of prostate cancer: preliminary findings. *J Magn Reson Imaging* 2014; **40**: 723-729 [PMID: 24924835 DOI: 10.1002/jmri.24379]

94 **Jensen JH**, Helpern JA. MRI quantification of non-Gaussian water diffusion by kurtosis analysis. *NMR Biomed* 2010; **23**: 698-710 [PMID: 20632416 DOI: 10.1002/nbm.1518]

95 **Malagi AV**, Das CJ, Khare K, Calamante F, Mehndiratta A. Effect of combination and number of b values in IVIM analysis with post-processing methodology: simulation and clinical study. *MAGMA* 2019; **32**: 519-527 [PMID: 31214819 DOI: 10.1007/s10334-019-00764-0]

96 **Malagi AV**, Netaji A, Kumar V, Baidya Kayal E, Khare K, Das CJ, Calamante F, Mehndiratta A. IVIM-DKI for differentiation between prostate cancer and benign prostatic hyperplasia: comparison of 1.5 T vs. 3 T MRI. *MAGMA* 2022; **35**: 609-620 [PMID: 34052899 DOI: 10.1007/s10334-021-00932-1]

97 **Bao J**, Wang X, Hu C, Hou J, Dong F, Guo L. Differentiation of prostate cancer lesions in the Transition Zone by diffusion-weighted MRI. *Eur J Radiol Open* 2017; **4**: 123-128 [PMID: 29034282 DOI: 10.1016/j.ejro.2017.08.003]

98 **Chang CB**, Lin YC, Wong YC, Lin SN, Lin CY, Lin YH, Sheng TW, Huang CC, Yang LY, Wang LJ. IVIM Parameters on MRI Could Predict ISUP Risk Groups of Prostate Cancers on Radical Prostatectomy. *Front Oncol* 2021; **11**: 659014 [PMID: 34277409 DOI: 10.3389/fonc.2021.659014]

99 **Liu Y**, Wang X, Cui Y, Jiang Y, Yu L, Liu M, Zhang W, Shi K, Zhang J, Zhang C, Li C, Chen M. Comparative Study of Monoexponential, Intravoxel Incoherent Motion, Kurtosis, and IVIM-Kurtosis Models for the Diagnosis and Aggressiveness Assessment of Prostate Cancer. *Front Oncol* 2020; **10**: 1763 [PMID: 33042822 DOI: 10.3389/fonc.2020.01763]

100 **Das CJ**, Malagi AV, Sharma R, Mehndiratta A, Kumar V, Khan MA, Seth A, Kaushal S, Nayak B, Kumar R, Gupta AK. Intravoxel incoherent motion and diffusion kurtosis imaging and their machine-learning-based texture analysis for detection and assessment of prostate cancer severity at 3 T. *NMR Biomed* 2024; **37**: e5144 [PMID: 38556777 DOI: 10.1002/nbm.5144]

101 **Kuru TH**, Roethke MC, Stieltjes B, Maier-Hein K, Schlemmer HP, Hadaschik BA, Fenchel M. Intravoxel incoherent motion (IVIM) diffusion imaging in prostate cancer - what does it add? *J Comput Assist Tomogr* 2014; **38**: 558-564 [PMID: 24733005 DOI: 10.1097/RCT.0000000000000088]

102 **Zhang YD**, Wang Q, Wu CJ, Wang XN, Zhang J, Liu H, Liu XS, Shi HB. The histogram analysis of diffusion-weighted intravoxel incoherent motion (IVIM) imaging for differentiating the gleason grade of prostate cancer. *Eur Radiol* 2015; **25**: 994-1004 [PMID: 25430007 DOI: 10.1007/s00330-014-3511-4]

103 **Yang DM**, Kim HC, Kim SW, Jahng GH, Won KY, Lim SJ, Oh JH. Prostate cancer: correlation of intravoxel incoherent motion MR parameters with Gleason score. *Clin Imaging* 2016; **40**: 445-450 [PMID: 27133684 DOI: 10.1016/j.clinimag.2016.01.001]

104 **Shan Y**, Chen X, Liu K, Zeng M, Zhou J. Prostate cancer aggressive prediction: preponderant diagnostic performances of intravoxel incoherent motion (IVIM) imaging and diffusion kurtosis imaging (DKI) beyond ADC at 3.0 T scanner with gleason score at final pathology. *Abdom Radiol (NY)* 2019; **44**: 3441-3452 [PMID: 31144091 DOI: 10.1007/s00261-019-02075-3]

105 **Panda A**, Gulani V, Ponsky LE. Reading MRI of the Prostate: A Practical Guide. Cham: Springer, 2020

106 **Ma D**, Gulani V, Seiberlich N, Liu K, Sunshine JL, Duerk JL, Griswold MA. Magnetic resonance fingerprinting. *Nature* 2013; **495**: 187-192 [PMID: 23486058 DOI: 10.1038/nature11971]

107 **Jiang Y**, Ma D, Seiberlich N, Gulani V, Griswold MA. MR fingerprinting using fast imaging with steady state precession (FISP) with spiral readout. *Magn Reson Med* 2015; **74**: 1621-1631 [PMID: 25491018 DOI: 10.1002/mrm.25559]

108 **Gibbs P**, Liney GP, Pickles MD, Zelhof B, Rodrigues G, Turnbull LW. Correlation of ADC and T2 measurements with cell density in prostate cancer at 3.0 Tesla. *Invest Radiol* 2009; **44**: 572-576 [PMID: 19692841 DOI: 10.1097/RLI.0b013e3181b4c10e]

109 **Simpkin CJ**, Morgan VA, Giles SL, Riches SF, Parker C, deSouza NM. Relationship between T2 relaxation and apparent diffusion coefficient in malignant and non-malignant prostate regions and the effect of peripheral zone fractional volume. *Br J Radiol* 2013; **86**: 20120469 [PMID: 23426849 DOI: 10.1259/bjr.20120469]

110 **Panda A**, O'Connor G, Lo WC, Jiang Y, Margevicius S, Schluchter M, Ponsky LE, Gulani V. Targeted Biopsy Validation of Peripheral Zone Prostate Cancer Characterization With Magnetic Resonance Fingerprinting and Diffusion Mapping. *Invest Radiol* 2019; **54**: 485-493 [PMID:

30985480 DOI: 10.1097/RLI.0000000000000569]

111 **Panda A**, Obmann VC, Lo WC, Margevicius S, Jiang Y, Schluchter M, Patel IJ, Nakamoto D, Badve C, Griswold MA, Jaeger I, Ponsky LE, Gulani V. MR Fingerprinting and ADC Mapping for Characterization of Lesions in the Transition Zone of the Prostate Gland. *Radiology* 2019; **292**: 685-694 [PMID: 31335285 DOI: 10.1148/radiol.2019181705]

112 **Yu AC**, Badve C, Ponsky LE, Pahwa S, Dastmalchian S, Rogers M, Jiang Y, Margevicius S, Schluchter M, Tabayoyong W, Abouassaly R, McGivney D, Griswold MA, Gulani V. Development of a Combined MR Fingerprinting and Diffusion Examination for Prostate Cancer. *Radiology* 2017; **283**: 729-738 [PMID: 28187264 DOI: 10.1148/radiol.2017161599]

113 **Davnall F**, Yip CS, Ljungqvist G, Selmi M, Ng F, Sanghera B, Ganeshan B, Miles KA, Cook GJ, Goh V. Assessment of tumor heterogeneity: an emerging imaging tool for clinical practice? *Insights Imaging* 2012; **3**: 573-589 [PMID: 23093486 DOI: 10.1007/s13244-012-0196-6]

114 **Miles KA**, Ganeshan B, Hayball MP. CT texture analysis using the filtration-histogram method: what do the measurements mean? *Cancer Imaging* 2013; **13**: 400-406 [PMID: 24061266 DOI: 10.1102/1470-7330.2013.9045]

115 **Schieda N**, Lim CS, Zabihollahy F, Abreu-Gomez J, Krishna S, Woo S, Melkus G, Ukwatta E, Turkbey B. Quantitative Prostate MRI. *J Magn Reson Imaging* 2021; **53**: 1632-1645 [PMID: 32410356 DOI: 10.1002/jmri.27191]

116 **Hameed M**, Ganeshan B, Shur J, Mukherjee S, Afaq A, Batura D. The clinical utility of prostate cancer heterogeneity using texture analysis of multiparametric MRI. *Int Urol Nephrol* 2019; **51**: 817-824 [PMID: 30929224 DOI: 10.1007/s11255-019-02134-0]

117 **Wibmer A**, Hricak H, Gondo T, Matsumoto K, Veeraraghavan H, Fehr D, Zheng J, Goldman D, Moskowitz C, Fine SW, Reuter VE, Eastham J, Sala E, Vargas HA. Haralick texture analysis of prostate MRI: utility for differentiating non-cancerous prostate from prostate cancer and differentiating prostate cancers with different Gleason scores. *Eur Radiol* 2015; **25**: 2840-2850 [PMID: 25991476 DOI: 10.1007/s00330-015-3701-8]

118 **Baek TW**, Kim SH, Park SJ, Park EJ. Texture analysis on bi-parametric MRI for evaluation of aggressiveness in patients with prostate cancer. *Abdom Radiol (NY)* 2020; **45**: 4214-4222 [PMID: 32740864 DOI: 10.1007/s00261-020-02683-4]

119 **Krishna S**, Lim CS, McInnes MDF, Flood TA, Shabana WM, Lim RS, Schieda N. Evaluation of MRI for diagnosis of extraprostatic extension in prostate cancer. *J Magn Reson Imaging* 2018; **47**: 176-185 [PMID: 28387981 DOI: 10.1002/jmri.25729]

120 **Xiong H**, He X, Guo D. Value of MRI texture analysis for predicting high-grade prostate cancer. *Clin Imaging* 2021; **72**: 168-174 [PMID: 33279769 DOI: 10.1016/j.clinimag.2020.10.028]

121 **Chu L**, Si Y, Liu RB. [The Value of MRI Texture Analysis in Identifying Intraductal Carcinoma of the Prostate Gland]. *Sichuan Da Xue Xue Bao Yi Xue Ban* 2020; **51**: 42-48 [PMID: 31950788 DOI: 10.12182/20200160101]

122 **Li M**, Guo J, Hu P, Jiang H, Chen J, Hu J, Asbach P, Sack I, Li W. Tomoelastography Based on Multifrequency MR Elastography for Prostate Cancer Detection: Comparison with Multiparametric MRI. *Radiology* 2021; **299**: 362-370 [PMID: 33687285 DOI: 10.1148/radiol.2021201852]

123 **Hu B**, Deng Y, Chen J, Kuang S, Tang W, He B, Zhang L, Xiao Y, Chen J, Rossman P, Arani A, Yin Z, Glaser KJ, Yin M, Venkatesh SK, Ehman RL, Wang J. Evaluation of MR elastography for prediction of lymph node metastasis in prostate cancer. *Abdom Radiol (NY)* 2021; **46**: 3387-3400 [PMID: 33651125 DOI: 10.1007/s00261-021-02982-4]

Published by **Baishideng Publishing Group Inc**
7041 Koll Center Parkway, Suite 160, Pleasanton, CA 94566, USA
Telephone: +1-925-3991568
E-mail: office@baishideng.com
Help Desk: https://www.f6publishing.com/helpdesk
https://www.wjgnet.com